NASA TECHNICAL NOTE

NASA TN D-3991

ELASTIC AND INELASTIC SCATTERING OF 42-MeV ALPHA PARTICLES FROM EVEN TELLURIUM ISOTOPES

by Regis F. Leonard, William M. Stewart, and Norton Baron

Lewis Research Center
Cleveland, Ohio

NATIONAL AERONAUTICS AND SPACE ADMINISTRATION • WASHINGTON, D. C. • MAY 1967

NASA TN D-3991

ELASTIC AND INELASTIC SCATTERING OF 42-MeV ALPHA PARTICLES FROM EVEN TELLURIUM ISOTOPES

By Regis F. Leonard, William M. Stewart, and Norton Baron

Lewis Research Center
Cleveland, Ohio

NATIONAL AERONAUTICS AND SPACE ADMINISTRATION

For sale by the Clearinghouse for Federal Scientific and Technical Information
Springfield, Virginia 22151 – CFSTI price $3.00

ELASTIC AND INELASTIC SCATTERING OF 42-MeV ALPHA PARTICLES FROM EVEN TELLURIUM ISOTOPES

by Regis F. Leonard, William M. Stewart, and Norton Baron

Lewis Research Center

SUMMARY

Angular distributions were measured for alpha elastic and inelastic scattering with isotopically enriched targets of tellurium 122, 124, 126, 128, and 130 by using the 42-MeV alpha beam of the NASA 60-inch cyclotron. In each isotope, three excited states exhibited relatively large cross sections. These were the one-phonon quadrupole state, the two-phonon state with spin and parity 4^+, and the one-phonon octupole state. Several other states were excited in each isotope but with cross sections that were too small to allow determination of very reliable excitation energies or differential cross sections.

The elastic angular distributions were analyzed by using the optical model with a four-parameter Woods-Saxon potential and the Blair sharp cutoff model. Optical model fits have been obtained for a wide range of values of optical model parameters. All potentials that give a satisfactory fit to the experimental data are nearly identical at their outer edges, although they vary widely in the interior of the nucleus. Sharp cutoff fits are typical of the type usually obtained.

Inelastically scattered groups of alpha particles were analyzed by using a distorted wave Born approximation (DWBA). These calculations yield excellent shape fits to the inelastic differential cross sections and allow the determination of deformation parameters that are in agreement with those measured by other methods.

INTRODUCTION

In a previous experiment, 40-MeV alpha particles were scattered from the even isotopes of tin (ref. 1). It was possible to excite collective states of the nucleus with relatively large cross sections, and to extract useful information concerning nuclear deformations and excitation energies. Tin is a rather special case, inasmuch as it possesses a closed proton shell. As a result of this condition, the excitation energies of the first vibrational level in the even tin nuclei are exceptionally high by comparison with other even-even nuclei in this region. The present work was undertaken to determine the dependence, if any, of other excitation energies and deformations on shell closure, therefore, the neighboring even-even nuclei to tin were selected, namely, those of tellurium.

When the present work was undertaken, both excitation energies and deformations were known for the quadrupole states (refs. 2 to 4). For the octupole states, however, very little information was available on either excitation energies or deformations. Recently published results (ref. 5) of inelastic deuteron scattering list excitation energies for the 3^- states in tellurium 124, 126, 128, and 130, as well as estimates of deformation parameters β_3 for tellurium 124, 128, and 130.

The data were analyzed by using the same methods as were applied to the tin isotopes reported in reference 1 - namely, the description of the elastic scattering in terms of an optical potential and the Blair sharp cutoff model, and the inelastic scattering in terms of the distorted wave Born approximation.

SYMBOLS

A	nuclear mass number
a	diffuseness parameter in Woods-Saxon potential
C_V	$V \exp(R_o A^{1/3}/a)$
C_W	$W \exp(R_o A^{1/3}/a)$
$d\sigma/d\Omega$	differential cross section, mb/sr
ΔE	energy loss, MeV
N	number of data points per differential cross section
R_o	nuclear radius constant
R_{sco}	radius constant for sharp cutoff model
r	semiclassical interaction radius
U	average optical potential
V	strength of real part of nuclear optical potential
V_c	coulomb potential
W	strength of imaginary part of nuclear optical potential
β	nuclear deformation parameter
θ_{cm}	center mass scattering angle, deg

ρt target thickness

σ total reaction cross section

χ^2 measure of statistical goodness of fit

EXPERIMENTAL ARRANGEMENT

The external 42-MeV alpha-particle beam of the NASA 60-inch cyclotron was used in this experiment in conjunction with a 64-inch-diameter scattering chamber. A schematic diagram of the external beam system is shown in figure 1. The deflected beam is mag-

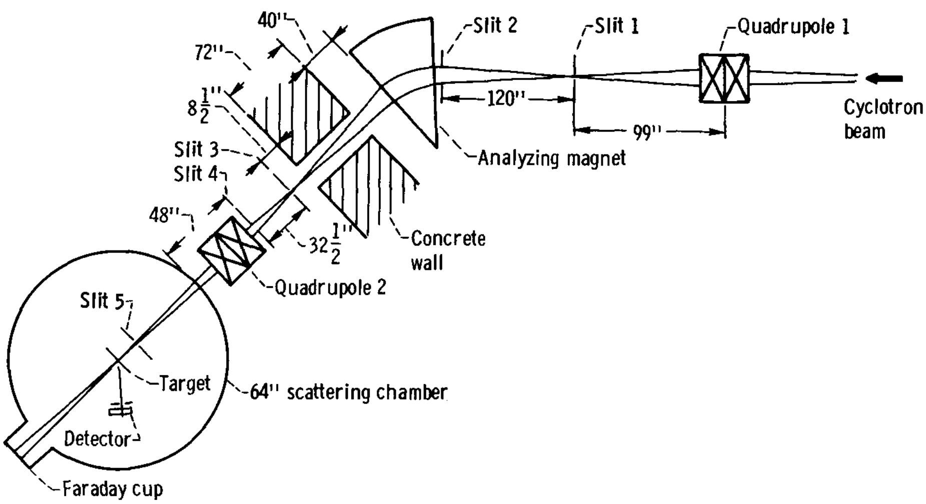

Figure 1. - Schematic diagram of experimental arrangement.

netically focused by quadrupole 1 onto slit 1. The acceptance angle into the analyzing magnet is controlled by slit 2. The analyzing magnet focuses the beam at slit 3, which together with slit 1 determines the energy spread of the beam incident on the target. The beam is refocused onto the target by quadrupole 2. Slits 4 and 5 serve as scraper slits.

The data for tellurium 122, 126, 128, and 130 were taken by using a four-counter mount which permitted cross sections to be measured at four angles simultaneously. Apertures in front of each counter defined the angular separation between the counters (4°) and the angular acceptance of individual counters (0.75°). The counters were lithium-drifted silicon produced at Lewis Research Center (ref. 6).

All other details of the scattering chamber were exactly as reported in reference 1.

A block diagram of the electronics is shown in figure 2. The routing system allows the output of each detector to be stored in 1024 channels of the pulse height analyzer. The ratio of the two scalers yields the fraction of counts missed as a result of analyzer dead time.

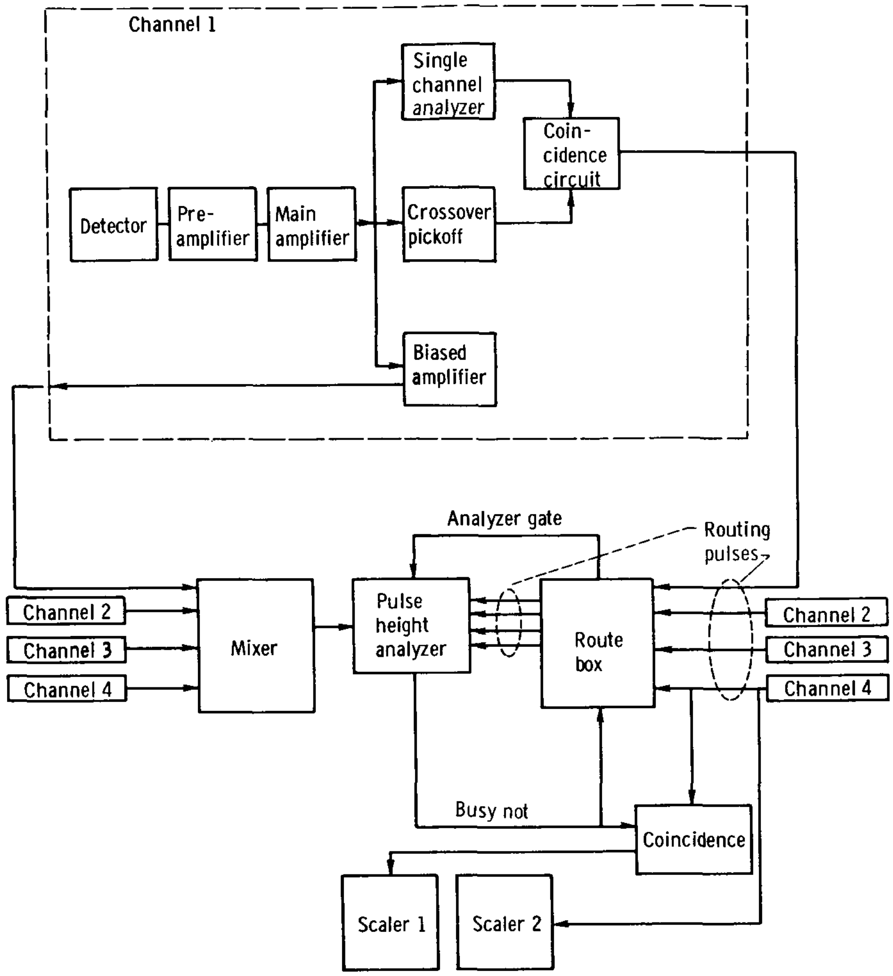

Figure 2. - Block diagram of electronics. (Channel 1 is shown in detail and is representative of channels 2, 3, and 4.)

The factors governing the energy resolution of the experiment are discussed in some detail in reference 1. Energy resolution of about 80-keV full width at half maximum could be obtained, but poorer resolution was often accepted in order to reduce the data-taking time. Overall resolution was usually between 80 and 120 keV.

The incident beam energy, determined by the method outlined in reference 1, was 42.0±0.20 MeV. The change in incident energy since the previously reported work is the result of a minor cyclotron modification.

EXPERIMENTAL RESULTS

States Excited by Inelastic Scattering

In each of the isotopes studied, three states were excited with relatively large cross sections, and a number of others were excited with somewhat smaller cross sections. Meaningful differential cross sections could be obtained only for the more strongly excited states. Excitation energies were obtained for all states that could be consistently identified. Excitation energies were determined by using (with kinematic corrections) the well known carbon 12 spectrum for calibration. Inasmuch as the targets were backed on carbon, the calibration and experiment could be performed simultaneously.

The lowest excited state in each tellurium isotope has a spin and parity 2^+ and is strongly excited. The excitation energies as determined here are consistent with previously measured results (refs. 3 and 4). As is usually the case for the quadrupole vibrational state, the differential cross section exhibits a structure typical of a diffraction phenomenon which is out of phase with the elastic differential cross section.

In addition to the quadrupole state, a fairly strong octupole state was observed in each isotope. The excitation energy is in agreement with that previously measured for tellurium 124, 126, 128, and 130 (ref. 5). The octupole state had not previously been observed in tellurium 122. As is usually the case, the octupole angular distribution is in phase with that of elastically scattered alpha particles. In each isotope, a peak was also seen at twice the energy of the first excited state, although its cross section was considerably smaller. The excitation energies, when compared with previous work (refs. 7 to 9), indicate that this peak is the 4^+ member of the two-phonon triplet. The 2^+ member of the triplet has been reported at an excitation energy such that it could barely have been resolved in the present experiment. Examination of the spectra of scattered alpha particles, however, does indicate in some cases a broadening of the 4^+ line, which suggests that the 2^+ is also present but weaker by probably a factor of two. The angular distribution for the two-phonon group was observed to be in phase with the elastic differential cross section, a reversal of the usual Blair phase rule. This reversal has been previously observed in the scattering of 44-MeV alpha particles with excitation of some, but not all, of the two-phonon states of the iron, nickel, and zinc nuclei (ref. 10).

Several other groups were seen in each isotope, but with cross sections too small to permit the determination of reliable differential cross sections or excitation energies. In many cases, these weaker groups are undoubtedly multiplets, as is apparent from examination of the energy spectra, typical examples of which are shown in figure 3. A summary of all the groups observed, their measured excitation energies, and their relative excitation strengths are shown in figure 4. The excitation energies for the more strongly excited states (2^+, 3^-, and 4^+) are accurate to approximately ±20 keV, while those for the more weakly excited groups are probably only accurate to about ±50 keV. States marked with an asterisk in figure 4 are most probably multiplets.

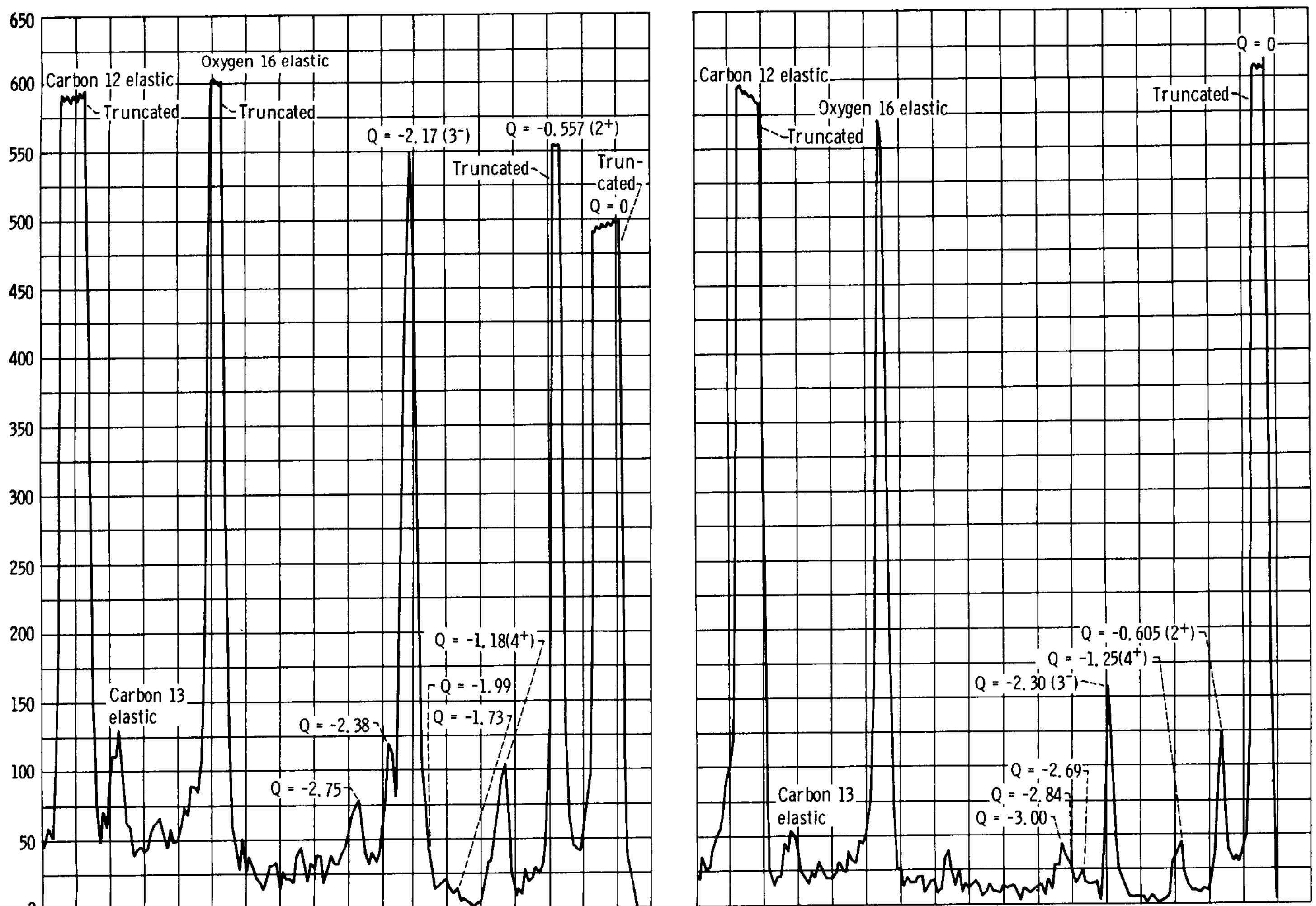

(a) Tellurium 122; scattering angle, 42°.

(b) Tellurium 124; scattering angle, 50°.

Figure 3. - Typical energy spectra.

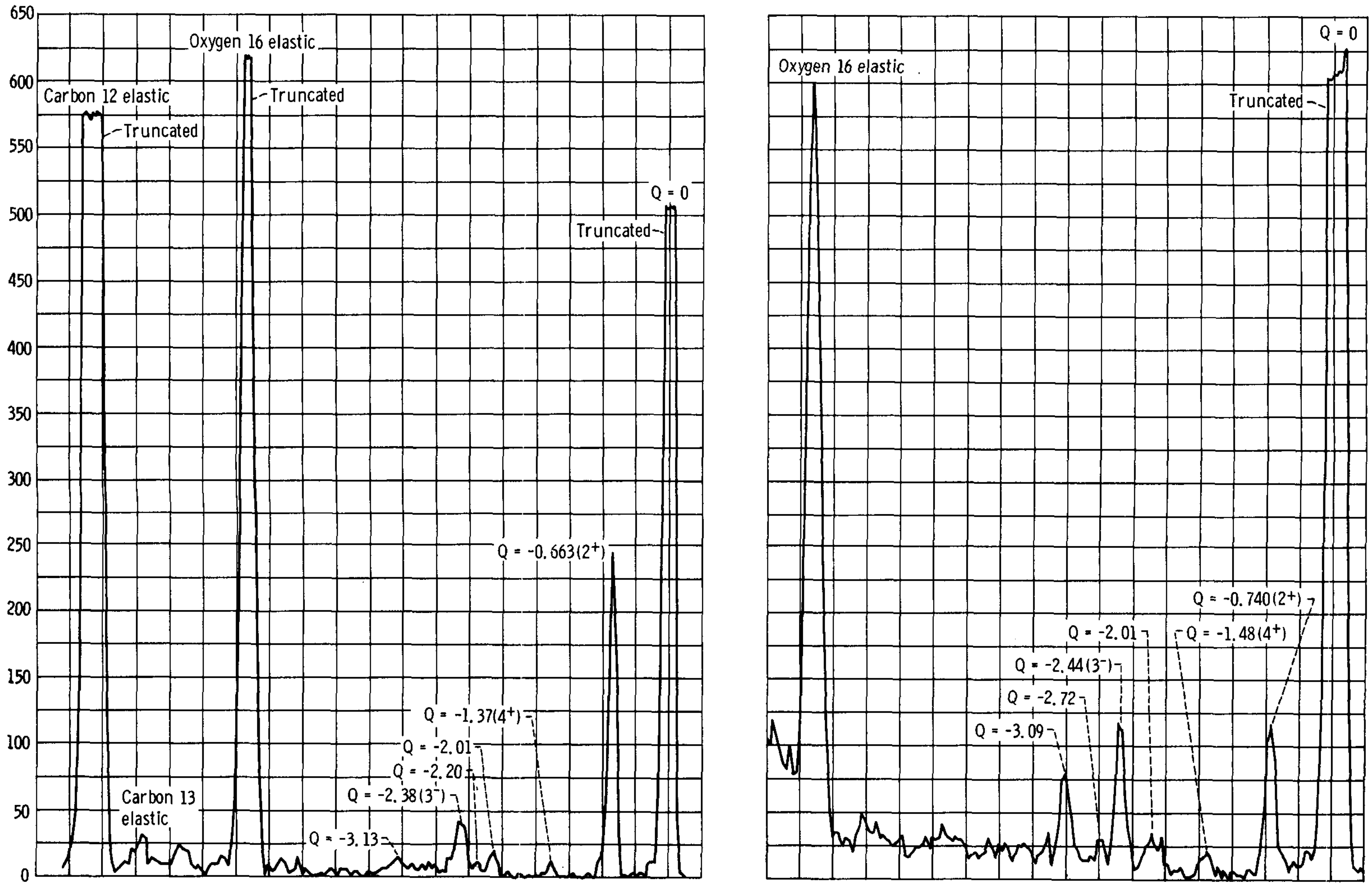

(c) Tellurium 126; scattering angle, 44°.

(d) Tellurium 128; scattering angle, 50°.

Figure 3. - Continued.

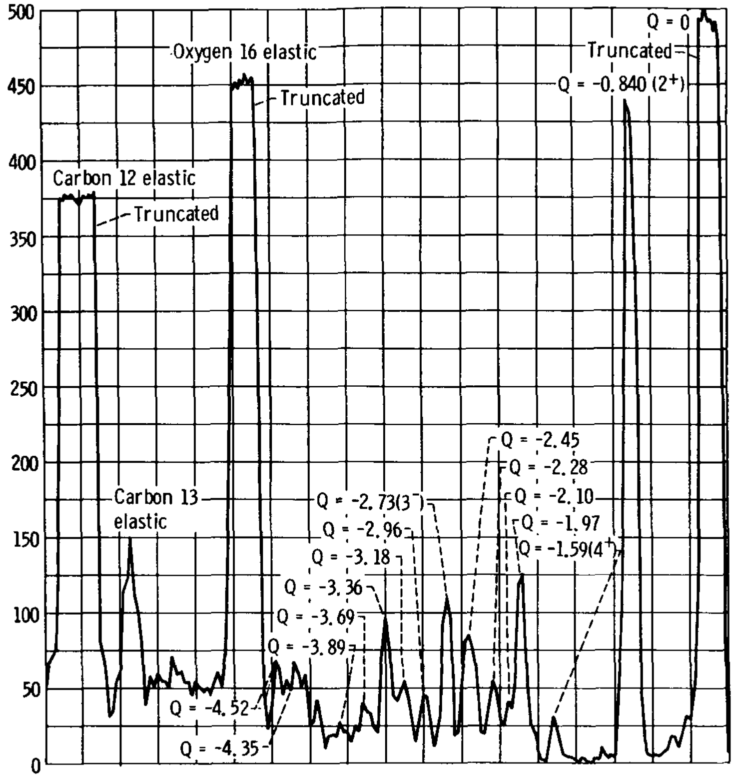

(e) Tellurium 130; scattering angle, 44°.

Figure 3. - Concluded.

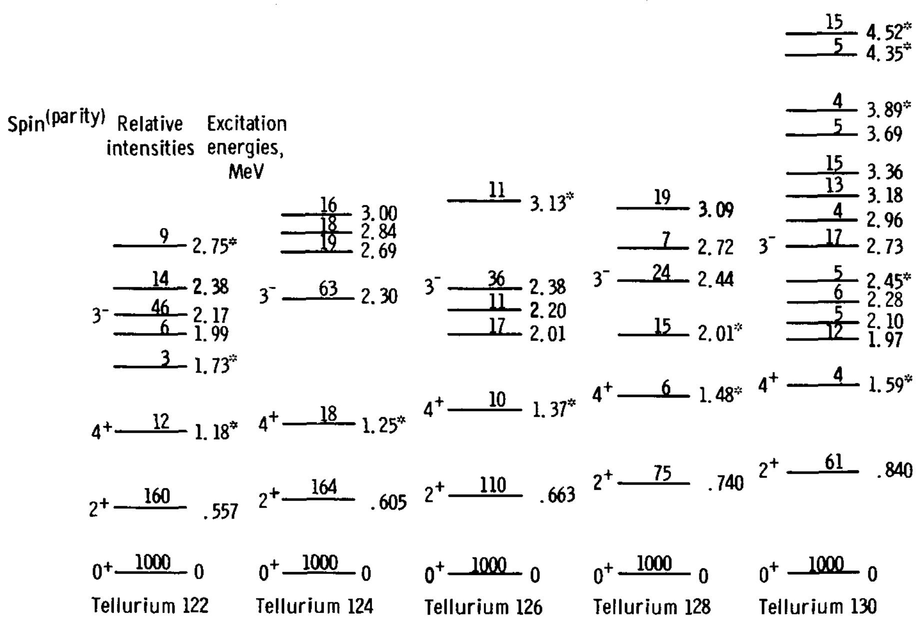

Figure 4. - Level diagram of tellurium isotopes. (The asterisk denotes probable multiplets.)

Cross Sections

Principal sources of error in the determination of absolute cross sections were inaccuracies in determining the number of scattered particles and in determining the target thickness. The intensity of scattered particles is made uncertain by the presence of background, which was estimated graphically and subtracted, and by the statistical uncertainty, which is listed with the compiled cross sections in appendix A.

The target thicknesses were calculated from the measured energy degradation of 8.78-MeV alpha particles from a naturally radioactive source. The principal uncertainty is in the calculated stopping power (ref. 11). The targets used in the present experiment were backed on 25 micrograms per centimeter squared of carbon. The measured thickness of all five targets, after correction for the carbon backing, is given in table I, both in units of the energy loss of 8.78-MeV alpha particles and in milligrams per centimeter squared as calculated by using reference 11. Also listed in table I are the isotopic enrichments as furnished by the supplier (Oak Ridge Laboratory Isotopes Development Center). Other small errors are contributed by imperfect measurement of the total incident charge and of the solid angle subtended by the detectors. The total error in the relative cross sections should be only 1 or 2 percent more than that due to statistical errors. The absolute cross sections will probably have an additional error of approximately 8 to 10 percent. All of the measured differential cross sections are shown (with statistical errors) in figure 5. A tabulation of the cross sections is contained in tables IV to VIII at the back of the report (pp. 22 to 28).

TABLE I. - TARGET DESCRIPTION

Tellurium isotope	Energy loss of 8.78 alpha particle, ΔE, keV	Target thickness, ρt, mg/cm^2	Isotopic enrichment
122	27.78	0.129	0.948
124	59.08	.274	.939
126	50.22	.233	.940
128	26.67	.124	.928
130	48.05	.223	.995

ANALYSIS OF ELASTIC SCATTERING DATA

The elastic scattering data were analyzed by using the optical model with a four-parameter Woods-Saxon potential given by

$$U(r) = -(V + iW)\left\{1 + \exp\left[\left(r - R_0A^{1/3}\right)/a\right]\right\}^{-1} + V_c \tag{1}$$

The computer program SCAT 4 was used to carry out the calculation of differential cross sections and total reaction cross sections (ref. 12). A brief account of the calculation as well as references to more detailed discussions of the optical model is given in reference 1.

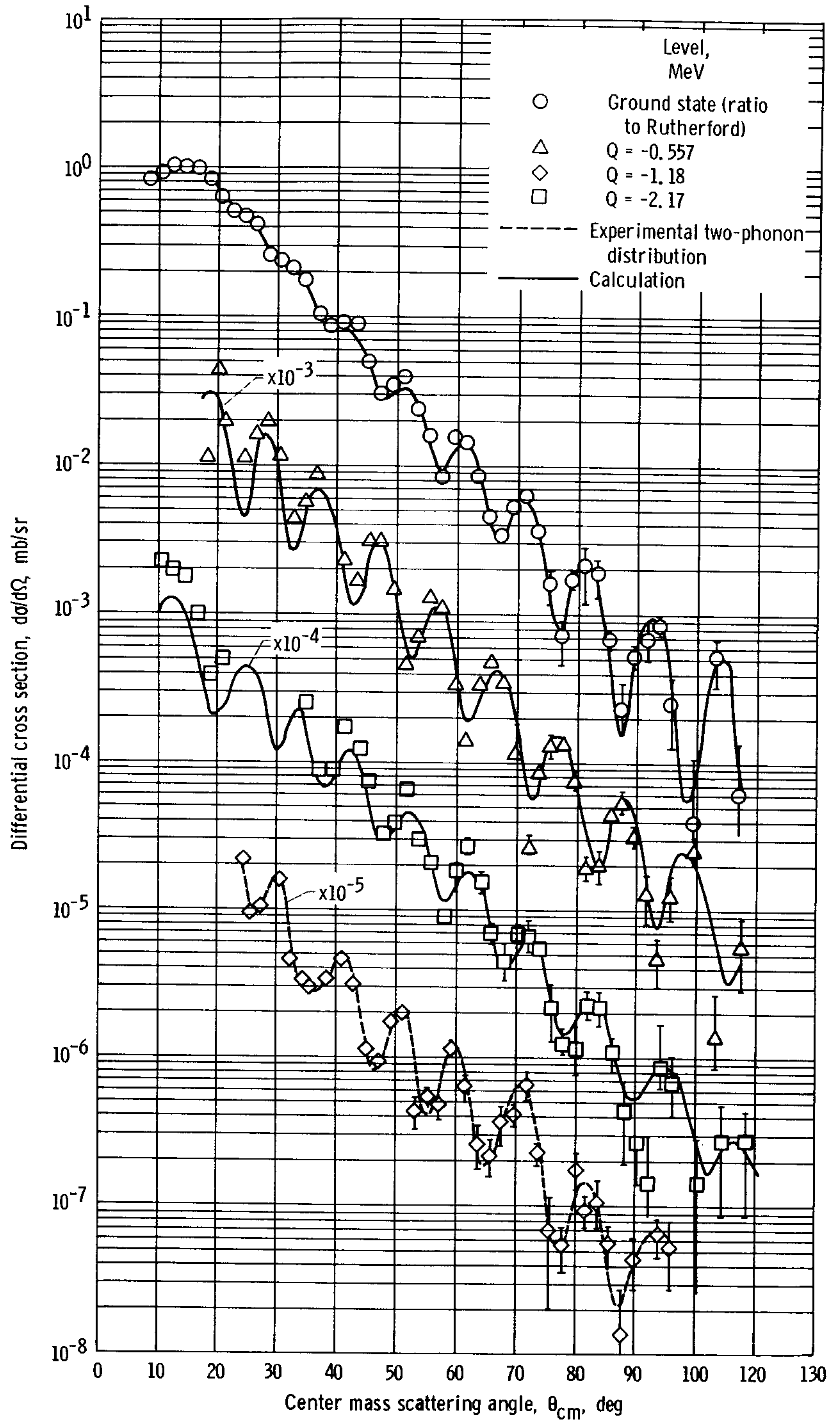

(a) Tellurium 122.

Figure 5. - Angular distributions for elastic and inelastic scattering of 42-MeV alpha particles.

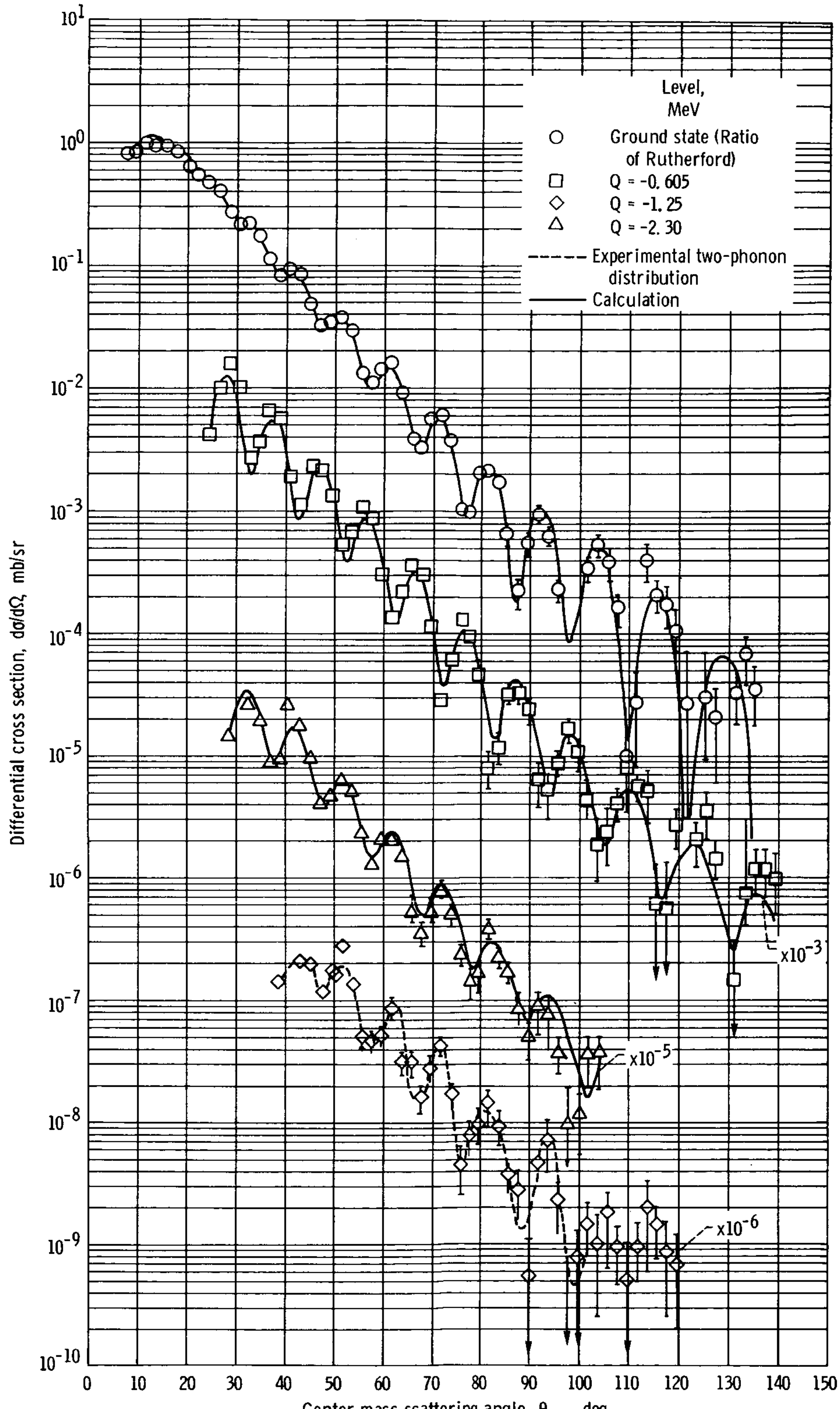

(b) Tellurium 124.

Figure 5. - Continued.

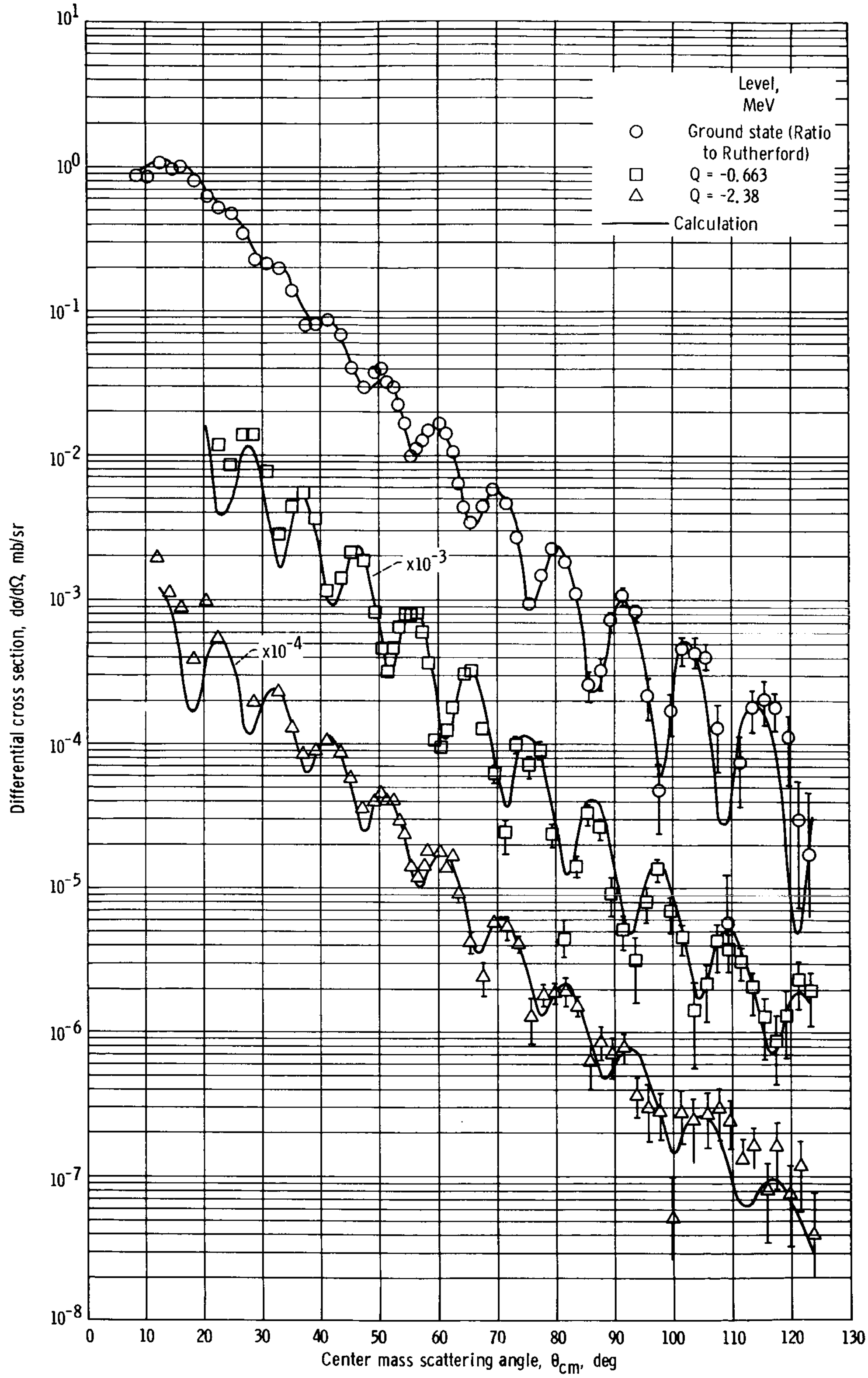

(c) Tellurium 126.

Figure 5. - Continued.

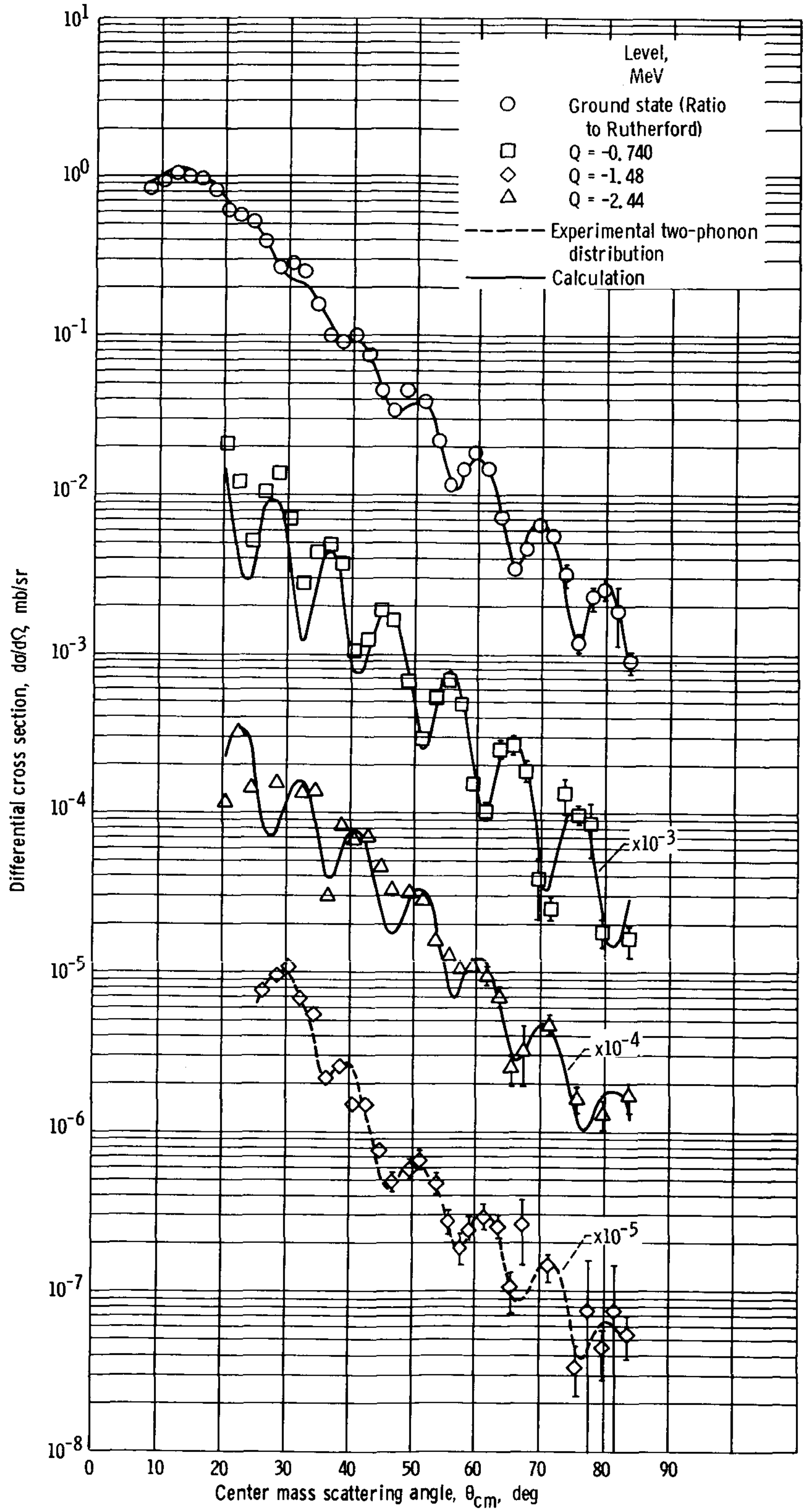

(d) Tellurium 128.

Figure 5. - Continued.

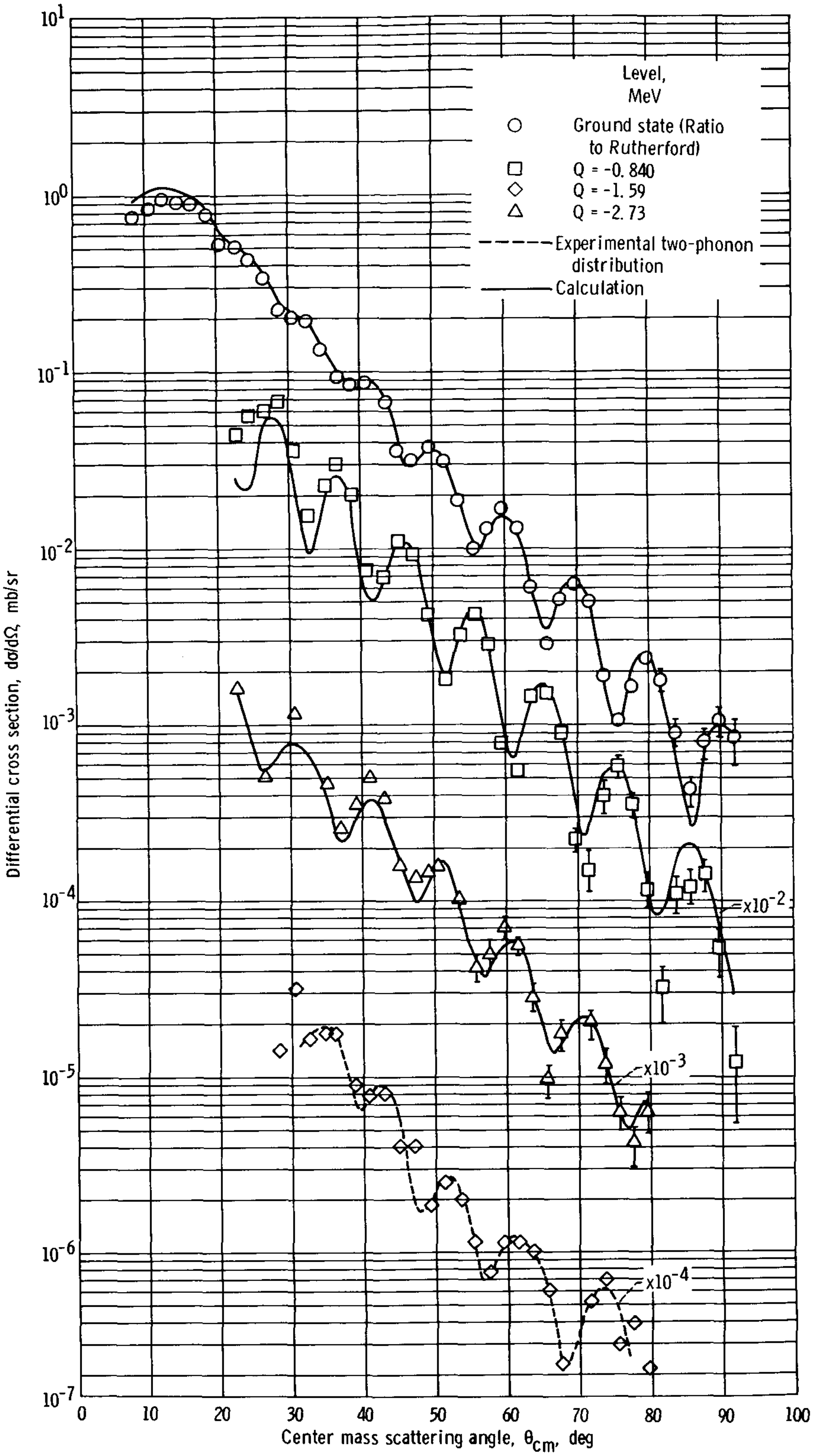

(e) Tellurium 130.

Figure 5. - Concluded.

In practice, the computer program was asked to minimize the quantity χ^2 by automatically searching on values of three of the optical model parameters (V, W, and a) while the fourth parameter R_0 remained fixed. If this process is repeated for various values of R_0, it is possible to obtain a reasonably good search of the four parameter space. A set of good parameters is shown (these are not necessarily the very best) together with calculated total reaction cross sections and χ^2/N for each isotope in table II. The theoretical cross sections, calculated by using the parameters of table II, are shown with the data in figure 5.

TABLE II. - ELASTIC SCATTERING ANALYSIS

Tellurium isotope	Strength of real part of nuclear optical potential, V, MeV	Strength of imaginary part of nuclear optical potential, W, MeV	Diffuseness parameter in Woods-Saxon potential, a, F	Nuclear radius constant, R_0, F	Total reaction cross section, σ_R, mb	Goodness of fit per data point, χ^2/N	Radius constant for sharp cutoff model, R_{sco}, F
122	36.64	19.95	0.671	1.50	1881	1.05	1.53
124	38.95	21.20	.672	1.48	1878	1.19	1.54
126	39.65	21.55	.682	1.48	1915	1.30	1.54
128	45.79	22.75	.655	1.48	1931	.67	1.53
130	34.13	20.19	.671	1.50	1959	1.76	1.55

As is usually the case with an optical model analysis of the scattering of medium energy alpha particles (ref. 1), there exists considerable ambiguity in the optical model parameters obtained. Austern (ref. 13) has proposed that the ambiguities arise from two sources, reflections from the nuclear interior and reflections from the surface. Drisko, Satchler, and Bassel (ref. 14) have discussed this possibility in some detail.

Waves reflected from the interior of two different potentials will have the same asymptotic form, and hence produce the same differential cross sections, if the potential depths allow one more half-wave length of the scattered particle within one potential well than within the other. This effect is most noticeable for low-numbered partial waves, which interact principally within the interior of the nucleus.

Those partial waves reflected at the nuclear surface, on the other hand, will produce the same differential cross section as long as the potential remains the same at the nuclear surface. This effect was first pointed out by Igo (ref. 15). The Woods-Saxon potential requires

$$Ve^{R_0A^{1/3}/a} = \text{constant} \equiv C_V \tag{2a}$$

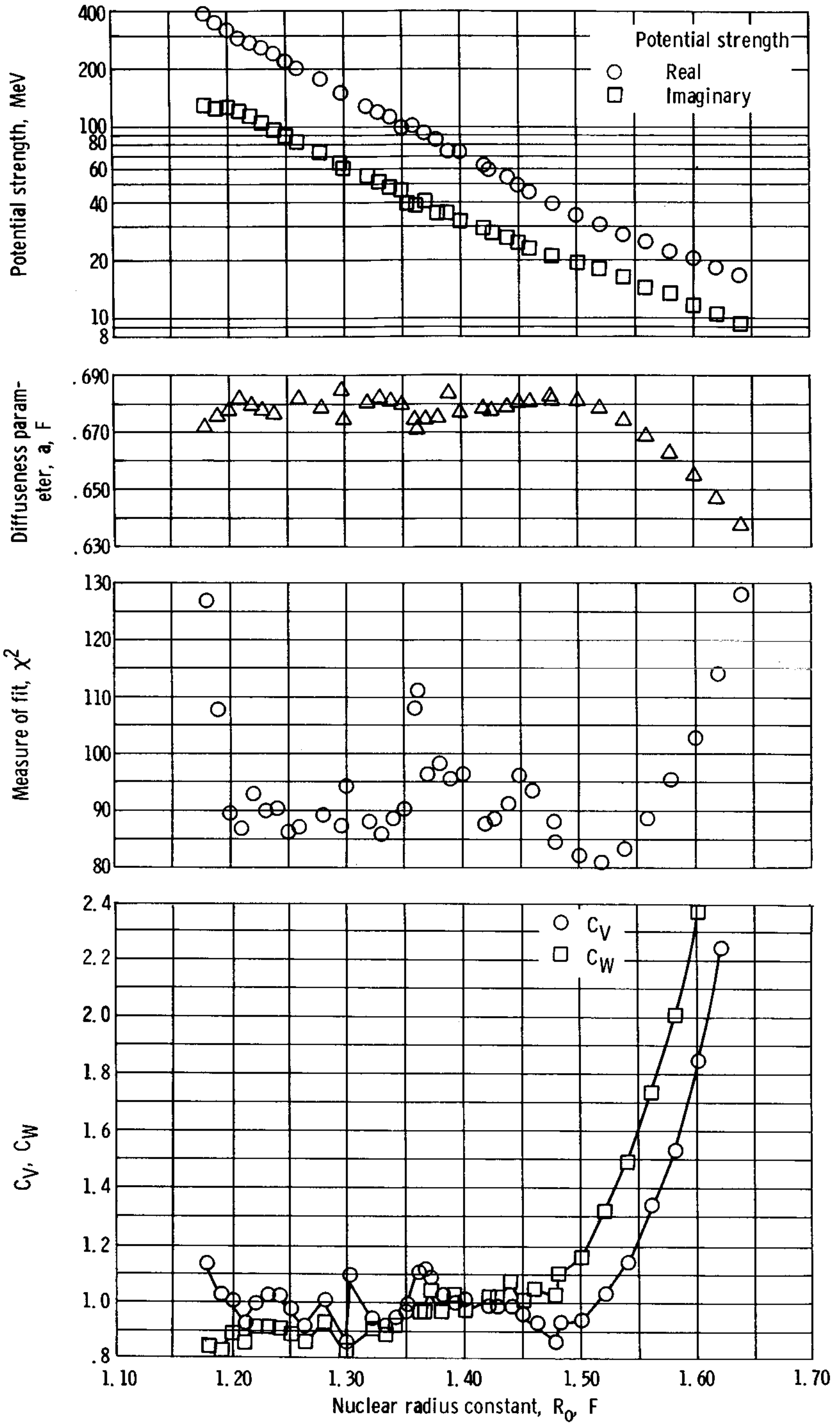

Figure 6. - Optical model parameters for tellurium 126.

$$We^{R_o A^{1/3}/a} = \text{constant} \equiv C_W \tag{2b}$$

$$a = \text{constant} \tag{2c}$$

It follows then that, if reflections from the nuclear interior are more important, the ambiguities in the optical model parameters will consist of a discrete set of well depths. If, however, reflection from the nuclear surface is more important, a continuous set of parameters should exist that satisfy equations (2). Drisko, Satcher, and Bassel have examined the scattering of 43-MeV alpha particles from nickel 58 and have found evidence that both effects are present.

In the present work, searches on the isotope tellurium 126 were carried out with a range of values of the optical model radius from 1.15 to 1.64. The optimum values of V, W, and a obtained for each radius are shown in figure 6 and listed in table IX (p. 29). Also plotted there (on a suppressed-zero scale) are values of χ^2 for each set of parameters, and the constants C_V and C_W. It is obvious that for $25 < V < 390$ MeV, V varies exponentially as R_o. A similar relation is true for W, while the diffuseness a is nearly independent of R_o. Computation of values of the constants C_V and C_W in equations (2a) and (2b) indicates that, except near the ends of the interval, C_V and C_W are constant to within about 15 percent. The constants C_V and C_W are also plotted in figure 6. Examination of the values of χ^2 shows that there are no very pronounced minima, such as would be anticipated if any discrete ambiguities existed. This indicates that the reflections from the interior of the nucleus are less important for scattering from tellurium than from nickel. This is similar to the results obtained in the scattering of 65-MeV alpha particles from zirconium (ref. 16) where only one pronounced minima in χ^2 was found. It would be expected that 40-MeV alphas would be more strongly absorbed than those of 65 MeV; hence, it is possible that no minima exist for the tellurium nucleus. In addition, it should be noted that the present work has attempted to fit data over a considerably wider angular range than was employed in either reference 15 or 16. Analysis of the elastic scattering was also carried out by using the Blair sharp cutoff model (ref. 17). The results of this analysis are shown in table II under the heading R_{sco} (R_{sco} is equal to the black disk radius divided by $A^{1/3}$).

ANALYSIS OF INELASTIC SCATTERING DATA

As in reference 1, the inelastic differential cross sections were compared with the predictions of a distorted wave Born approximation (DWBA). The calculation was carried out by using the direct-reaction-calculation code of Gibbs, et al. (ref. 18) with a surface interaction. The theoretical cross sections are shown with the data in figure 5. The fits

TABLE III. - ANALYSIS OF INELASTIC SCATTERING

Tellurium isotope	Nuclear deformation parameters					
	Present work		Previous work			
	β_2	β_3	β_2	$\beta_{2,ref}$	β_3	$\beta_{3,ref}$
122	0.20	0.11	0.19	2	----	---
124	.18	.13	.14	2	0.07	5
126	.17	.11	.163	3	.12	8
128	.15	.08	.141	3	.10	5
130	.12	.06	.127	3	.11	5

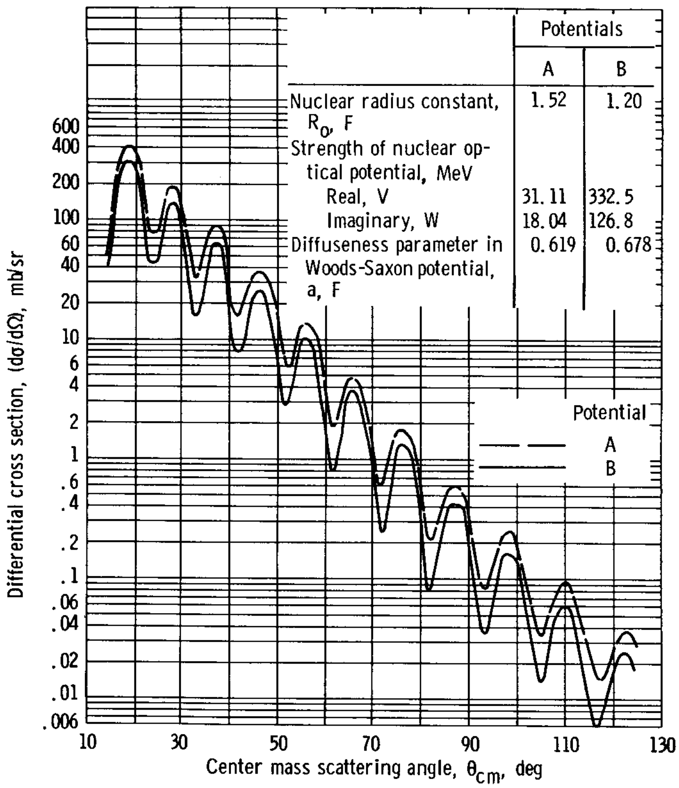

Figure 7. - Inelastic cross sections calculated by two different optical potentials for tellurium 126 in 2^+ state.

appear to be excellent. The only adjustable parameter involved in this calculation is the magnitude of the cross section. The normalization factor between theoretical and experimental cross sections permits the determination of the nuclear deformation in the excited state. The deformations so determined are listed in table III. Also shown there are previously measured deformations, obtained by using the methods of the Coulomb excitation of inelastic deuteron scattering. The agreement for all isotopes is good and comparable to that usually obtained.

One piece of information necessary as input for the direct reaction calculation is the set of optical model parameters determined from the elastic scattering. It is interesting to examine the inelastic scattering to see the effect of optical model ambiguities on the cross sections calculated by the direct-reaction-calculation program. For this purpose, the scattering to the first excited state of tellurium 126 was examined by using widely varying sets of optical model parameters obtained from the elastic scattering. It was found that the shape calculated for the inelastic cross section was only slightly dependent on the optical model parameters, while the magnitude (and, hence, the value of deformation) is slightly more sensitive to the potential used. That is shown in figure 7 where the cross sections calculated by using two different sets of parameters are plotted as functions of angle. The deformation parameter β changed from 0.16 for potential A to 0.20 for potential B.

It may be noted that only the quadrupole and octupole states have been analyzed with the direct-reaction-calculation code. The two-phonon states cannot be described by the simple form of the DWBA calculation involved here. The excitation of two-phonon states occurs, in part at least, by a two-step process, which sometimes results in the reversal of phase of the differential cross section seen here. It is necessary to employ a coupled-channels-type calculation in order to describe effectively such processes. Pramila, et al. (ref. 8) have done such calculations for the inelastic scattering of protons from tellurium 126 and have obtained satisfactory fits to experimental data.

CONCLUSIONS

An investigation of elastic and inelastic scattering of 42-MeV alpha particles from even tellurium isotopes revealed the following:

1. Excitation strengths: The present experiment has demonstrated the well known fact that the states most strongly excited in inelastic scattering are those described as collective states. In particular, the one-phonon 2^+, the one-phonon 3^-, and the two-phonon 4^+ are strongly excited in alpha-particle scattering.

2. Blair phase rule: The differential cross sections for excitation of both one-phonon states obey the Blair phase rule. The reverse of the usual phase rule is seen for the two-phonon states in all the tellurium isotopes.

3. Optical model analysis: Optical model analysis of elastic scattering exhibits ambiguities of a type which have been previously discussed by other authors. The continuous set of good parameters found here has never been seen before; however, this is presumably because such an analysis has never been done for the scattering of 42-MeV alpha particles from a nucleus as heavy as tellurium. Excellent fits to the experimental data could be obtained for all the isotopes. The inelastic scattering was fitted very well by the direct reaction calculation, with values of the nuclear deformation parameter derived that are in good agreement with those obtained in Coulomb excitation and inelastic deuteron scattering.

The direct-reaction-calculation cross sections varied slightly with considerable variations in the parameters of the distorting potential.

4. Effects of shell closure: It is well known that the excitation energies of quadrupole states are exceptionally high at closed shells. No such systematic variation of the octupole excitation energies has been apparent. The present work demonstrates that the octupole states seem far less sensitive to shell closure. The octupole energies in the tellurium isotopes are, in fact, almost equal to those of the tin isotopes, whereas the quadrupole energies for tellurium are approximately half of those seen in tin.

The deformation parameters for the quadrupole states of tellurium show a marked decrease with increasing neutron number, in contrast with those of tin, which are practically independent of mass number. In magnitude, the tellurium quadrupole deformations are somewhat larger than those of tin. The octupole deformation parameters show a similar tendency to decrease with increasing neutron number, although somewhat erratically. In tin, on the other hand, the octupole deformations were again virtually independent of mass number, and, for the most part, somewhat larger than those for tellurium.

The elastic cross sections for the tellurium isotopes are virtually identical, both in shape and magnitude, not only to each other, but also to the tin elastic cross sections as well. The small differences are to be expected and attributed to the small changes in mass, beam energy, or nuclear charge between the various isotopes of tin and tellurium.

Lewis Research Center,
National Aeronautics and Space Administration,
Cleveland, Ohio, October 26, 1966,
129-02-04-06-22.

REFERENCES

1. Baron, Norton; Leonard, Regis F.; Need, John L.; and Stewart, William M.: Elastic and Inelastic Scattering of 40-MeV Alpha Particles from Even Tin Isotopes. NASA TN D-3067, 1965.
2. Kisslinger, Leonard S.; and Sorensen, Raymond A.: Spherical Nuclei with Simple Residual Forces. Rev. Mod. Phys., vol. 35, no. 4, Oct. 1963, pp. 853-915.
3. Stelson, P. H.; and McGowan, F. K.: Coulomb Excitation of Medium-Weight Even-Even Nuclei. Phys. Rev., vol. 110, No. 2, Apr. 15, 1958, pp. 489-506.
4. Nuclear Data Group: Nuclear Data Sheet Nos. NRC-60-4-85; NRC-60-6-76; NRC-60-6-104; NRC-61-1-83; NRC-61-108. Oak Ridge Nat. Lab., 1965.
5. Kim, Y. S.; and Cohen, B. L.: Studies of (d, d) Reactions on Sn, Cd, Te, and Mo Isotopes. Phys. Rev., vol. 142, no. 3, Feb. 18, 1966, pp. 788-798.
6. Baron, Norton; and Kaminski, Gerald A.: Manufacture of Lithium-Drifted Silicon Surface-Barrier Simiconductor Counters. NASA TN D-3432, 1966.
7. Cookson, J. A.; and Darcey, W.: Collective Levels in the Even Isotopes of Cd and Te. Nucl. Phys., vol. 62, 1965, pp. 326-336.
8. Pramila, G. C.; Middleton, R.; Tamura, T.; and Satchler, G. R.: Proton Excitation of Vibrational States of ^{126}Te. Nucl. Phys., vol. 61, 1965, pp. 448-456.

9. Sakai, Mitsue; Yamazaki, Toshimitsu; and Ejiri, Hiroyasu H.: Measurement of Conversion Electrons from (p, 2n) Reactions on the Vibrational Nuclei. Nucl. Phys., vol. 74, 1965, pp. 81-109.

10. Faraggi, H.; and Saudinos, J.: Spectroscopic Data Deduced from Inelastic Scattering of 44-MeV Alpha Particles in Medium-Weight Nuclei. Nuclear Spectroscopy with Direct Reactions. I - Contributed Papers. F. E. Throw, ed., Rep. No. ANL-6848, Mar. 1964, pp. 137-142.

11. Williamson, C.; and Boujot, J. P.: Tables of Range and Rate of Energy Loss of Charged Particles of Energy 0.5 to 150 MeV. Rep. No. CEA-2189, Commissariat à e'Énergie Atomique, Centre d'Études Nucléaires, Saclay, 1963.

12. Melkanoff, Michel A.; Nodvik, John S.: Saxon, David S.; and Cantor, David G.: A FORTRAN Program for Elastic Scattering Analyses with the Nuclear Optical Model. University of California Press, 1961.

13. Austern, N.: Optical Model Wave Functions for Strongly Absorbing Nuclei. Annals Phys., vol. 15, no. 3, Sept. 1961, pp. 299-313.

14. Drisko, R. M.; Satchler, G. R.; and Bassel, R. H.: Ambiguities in the Optical Potential for Strongly Absorbed Projectiles. Phys. Letters, vol. 5, no. 5, Aug. 1, 1963, pp. 347-350.

15. Igo, George: Optical-Model Analysis of Excitation Function Data and Theoretical Reaction Cross Sections for Alpha Particles. Phys. Rev., vol. 115, no. 6, Sept. 15, 1959, pp. 1665-1674.

16. Bingham, C. R.; Halbert, M. L.; and Bassel, R. H.: Nuclear-Reaction Studies with 65-MeV Alpha Particles on Zirconium. Phys. Rev., vol. 148, no. 3, Aug. 19, 1966, pp. 1174-1191.

17. Blair, John S.: Inelastic Diffraction Scattering. Phys. Rev., vol. 115, no. 4, Aug. 15, 1959, pp. 928-938.

18. Gibbs, W. R.; Madsen, V. A.; Miller, J. A.; Tobocman, W.; Cox, E. C.; and Mowry, L.: Direct Reaction Calculation. NASA TN D-2170, 1964.

TABLE IV. - DIFFERENTIAL CROSS SECTION FOR SCATTERING OF 42-MeV ALPHA PARTICLES FROM TELLURIUM 122

(a) Elastic scattering

Center mass scattering angle, θ_{cm}, deg	Differential cross section, $d\sigma/d\Omega$, mb/sr	Center mass scattering angle, θ_{cm}, deg	Differential cross section, $d\sigma/d\Omega$, mb/sr	Center mass scattering angle, θ_{cm}, deg	Differential cross section, $d\sigma/d\Omega$, mb/sr
8.26	266000±650	32.79	286±2	67.52	0.315±0.032
10.12	139000±230	34.85	190±0.4	69.54	.445±0.017
10.32	123000±440	36.90	89.9±0.8	71.57	.480±0.039
12.18	77600±170	38.95	62.7±0.2	73.59	.252±0.013
14.25	41400±120	41.00	53.5±0.6	75.61	.098±0.018
14.45	34300±230	43.05	43.2±0.2	77.62	.0404±0.0051
16.31	21200±45	45.10	19.9±0.2	79.64	.0872±0.0106
16.51	20000±178	47.15	10.7±0.1	81.65	.105±0.008
18.38	12600±18	49.19	10.2±0.3	83.66	.0837±0.0104
18.58	10700±130	51.24	9.90±0.11	85.67	.0286±0.0041
20.44	6250±19	53.28	5.17±0.12	89.68	.0192±0.0034
20.64	5290±92	55.32	3.07±0.06	91.68	.0234±0.0055
22.50	3580±10	57.36	1.36±0.06	93.68	.0271±0.0040
24.56	2030±5	59.39	2.26±0.06	95.68	.0075±0.0031
26.62	1290±6	61.43	1.84±0.07	103.64	.0126±0.0040
28.68	587±3	63.46	.969±0.055	107.61	.0013±0.0013
30.73	418±0.5	65.49	.360±0.031		

(b) Inelastic scattering, 0.557-MeV level

18.38	11.4±0.6	47.16	3.14±0.06	75.62	0.124±0.020
20.44	41.4±1.6	49.20	1.43±0.10	77.64	.130±0.009
22.50	19.4±0.7	51.25	.455±0.024	79.65	.070±0.009
24.56	11.2±0.4	53.29	.696±0.043	81.66	.0181±0.0034
26.62	16.2±0.7	55.33	1.29±0.04	83.68	.0190±0.0051
28.68	20.0±0.5	57.37	1.08±0.05	85.68	.0427±0.0052
30.74	11.50±0.09	59.40	.329±0.020	87.69	.0519±0.0084
32.80	4.36±0.25	61.44	.131±0.019	89.69	.0297±0.0043
34.85	5.65±0.07	63.47	.337±0.033	91.69	.0123±0.0041
36.91	8.87±0.23	65.50	.481±0.027	93.69	.0044±0.0017
38.96	5.96±0.07	67.53	.332±0.033	95.69	.0119±0.0040
41.01	2.31±0.13	69.55	.110±0.009	99.68	.0238±0.0056
43.06	1.65±0.04	71.58	.0267±0.0094	103.65	.0013±0.0013
45.12	3.08±0.15	73.60	.0822±0.0074	107.62	.0054±0.0027

TABLE IV. - Concluded. DIFFERENTIAL CROSS SECTION FOR SCATTERING OF 42-MeV ALPHA PARTICLES FROM TELLURIUM 122

(c) Inelastic scattering, 1.183-MeV level

Center mass scattering angle, θ_{cm}, deg	Differential cross section, $d\sigma/d\Omega$, mb/sr	Center mass scattering angle, θ_{cm}, deg	Differential cross section, $d\sigma/d\Omega$, mb/sr	Center mass scattering angle, θ_{cm}, deg	Differential cross section, $d\sigma/d\Omega$, mb/sr
14.26	31.5±0.3	47.17	0.091±0.011	73.62	0.0225±0.0039
24.57	2.17±0.17	49.22	.175±0.032	75.64	.0067±0.0047
26.63	.962±0.163	51.26	.209±0.016	77.65	.0053±0.0019
28.69	1.01±0.12	53.30	.0433±0.0108	79.67	.0176±0.0049
30.75	1.38±0.03	55.34	.0538±0.0082	81.68	.0094±0.0024
30.75	1.79±0.22	57.38	.0489±0.0115	83.69	.0109±0.0038
32.81	.450±0.083	59.42	.117±0.012	85.70	.0057±0.0019
34.86	.343±0.016	61.45	.0628±0.0131	87.71	.0014±0.0014
36.92	.307±0.042	63.48	.0264±0.0094	89.71	.0044±0.0017
38.97	.342±0.016	65.51	.0216±0.0059	93.71	.0063±0.0020
41.02	.469±0.052	67.54	.0365±0.0110	95.71	.0053±0.0026
43.07	.311±0.015	69.57	.0429±0.0053	103.67	.0013±0.0013
45.12	.1128±0.0244	71.59	.0667±0.0149		

(d) Inelastic scattering, 2.168-MeV level

10.13	22.3±2.9	51.28	0.633±0.028	77.68	0.0113±0.0028
12.20	19.5±2.7	53.32	.287±0.028	79.69	.0108±0.0038
14.26	17.8±2.5	55.36	.196±0.016	81.70	.0219±0.0037
16.33	9.91±0.99	57.40	.0815±0.0149	83.72	.0204±0.0053
18.39	3.83±0.32	59.44	.171±0.015	85.72	.0101±0.0025
20.46	4.98±0.54	61.47	.254±0.026	87.73	.0041±0.0024
34.88	2.41±0.04	63.51	.142±0.022	89.73	.0025±0.0013
36.93	.762±0.066	65.54	.065±0.010	91.73	.0014±0.0014
38.99	.860±0.025	67.56	.043±0.012	93.73	.0083±0.0023
41.04	1.66±0.12	69.59	.066±0.007	95.73	.0066±0.0029
43.09	1.18±0.03	71.62	.063±0.015	99.72	.0013±0.0013
45.14	.703±0.062	73.64	.050±0.006	103.69	.0027±0.0019
47.19	.320±0.020	75.66	.020±0.008	107.66	.0027±0.0019
49.23	.377±0.046				

TABLE V. - DIFFERENTIAL CROSS SECTION FOR SCATTERING OF 42-MeV ALPHA

PARTICLES FROM TELLURIUM 124

(a) Elastic scattering

Center mass scattering angle, θ_{cm}, deg	Differential cross section, $d\sigma/s\Omega$, mb/sr	Center mass scattering angle, θ_{cm}, deg	Differential cross section, $d\sigma/d\Omega$, mb/sr	Center mass scattering angle, θ_{cm}, deg	Differential cross section, $d\sigma/d\Omega$, mb/sr
7.72	333000±2020	51.14	9.45±0.21	93.33	0.0173±0.0023
9.78	133000±807	53.18	6.07±0.09	95.72	.0083±0.0017
11.85	74500±595	55.22	2.34±0.05	97.76	0
13.91	36700±405	57.26	1.72±0.05	99.70	.0044±0.0013
15.97	20900±150	59.29	2.05±0.05	101.69	.0081±0.0020
18.03	11900±113	61.33	1.97±0.05	103.68	.0116±0.0021
20.10	5820±78	63.36	1.03±0.04	105.67	.0055±0.0016
22.16	3410±60	65.39	.381±0.021	107.65	.0033±0.0009
24.22	2150±45	67.42	.284±0.018	109.63	.0004±0.0004
26.53	1240±2	69.44	.461±0.023	111.61	.00049±0.00034
28.59	623±2	71.47	.463±0.016	113.59	.0068±0.0027
30.65	368±1	73.49	.245±0.013	115.56	.0034±0.0013
32.70	296±1	75.51	.0613±0.0072	117.53	.0028±0.0011
34.76	184.0±0.5	77.52	.0523±0.0069	119.51	.0016±0.0007
36.81	94.3±0.4	79.54	.101±0.009	121.47	.00039±0.00037
38.86	57.6±0.3	81.55	.0947±0.0120	123.44	0
40.91	52.9±0.3	83.56	.0720±0.0062	125.41	.00042±0.00042
42.96	38.7±0.2	85.57	.0260±0.0032	127.37	.000268±0.000189
45.01	19.2±0.2	87.58	.0079±0.0021	131.29	.00041±0.00024
47.05	10.7±0.1	89.58	.0182±0.0031	135.20	.000418±0.000241
49.10	9.69±0.11	91.58	.0309±0.0039		

(b) Inelastic scattering, 0.605-MeV level

24.48	4.05±0.14	67.43	0.300±0.019	109.64	0.0079±0.0025
26.54	9.84±0.22	69.45	.116±0.012	111.62	.0057±0.0015
28.60	15.4±0.3	71.48	.0282±0.0077	113.60	.0052±0.0022
30.65	8.85±0.11	73.50	.0594±0.0066	115.57	.00061±0.00051
32.71	2.64±0.06	75.52	.125±0.011	117.55	.00057±0.00057
34.76	3.57±0.07	77.54	.094±0.008	119.52	.00272±0.00096
36.32	6.38±0.09	79.55	.0461±0.0064	123.45	.0021±0.0007
38.87	5.50±0.09	81.56	.0076±0.0036	125.42	.0036±0.0015
40.92	1.85±0.05	83.57	.0115±0.0026	127.38	.00143±0.00045
42.97	1.09±0.04	85.58	.0307±0.0036	131.30	.00015±0.00015
45.02	2.27±0.06	87.59	.0314±0.0042	133.26	.00074±0.00033
47.06	2.08±0.05	89.59	.0238±0.0036	135.21	.00119±0.00042
49.11	1.28±0.04	91.59	.00502±0.00240	137.17	.00120±0.00042
51.20	.527±0.023	93.73	.0051±0.0029	139.12	.00103±0.00046
53.19	.669±0.029	95.72	.0088±0.0018	141.07	.00046±0.00026
55.23	1.04±0.04	97.72	.0166±0.0039	143.02	.00031±0.00022
57.27	.867±0.034	99.72	.0102±0.0020	144.97	0
59.31	.298±0.020	101.71	.0044±0.0017	146.92	.00016±0.00016
61.34	.139±0.018	103.69	.0019±0.0009	148.86	.00016±0.00016
63.37	.215±0.017	105.68	.0024±0.0013	150.81	.0011±0.0004
65.40	.362±0.022	107.66	.0041±0.0013		

TABLE V. - Concluded. DIFFERENTIAL CROSS SECTION FOR SCATTERING OF 42-MeV ALPHA PARTICLES FROM TELLURIUM 124

(c) Inelastic scattering, 1.245-MeV level

Center mass scattering angle, θ_{cm}, deg	Differential cross section, $d\sigma/d\Omega$, mb/sr	Center mass scattering angle, θ_{cm}, deg	Differential cross section, $d\sigma/d\Omega$, mb/sr	Center mass scattering angle, θ_{cm}, deg	Differential cross section, $d\sigma/d\Omega$, mb/sr
38.88	0.142±0.014	69.47	0.0274±0.0058	95.61	0.00230±0.00094
42.98	.206±0.017	71.49	.0430±0.0041	97.60	0
45.03	.195±0.016	73.52	.0161±0.0034	99.59	.000782±0.00055
47.08	.119±0.013	75.54	.00453±0.0020	101.58	.00145±0.0010
49.12	.170±0.015	77.55	.00778±0.0025	103.57	.000979±0.00057
51.16	.271±0.017	79.57	.00974±0.0029	105.56	.00182±0.0014
53.21	.136±0.013	81.58	.0137±0.0033	107.54	.000940±0.00054
55.25	.050±0.008	83.59	.00922±0.0023	109.52	.000402±0.00040
57.28	.0473±0.0079	85.60	.00384±0.0013	111.50	.000922±0.00082
59.32	.0521±0.0082	87.61	.00280±0.0012	113.48	.00207±0.0015
61.35	.0853±0.0101	89.61	.000553±0.00055	115.45	.00142±0.00081
63.39	.0307±0.0063	91.61	.00464±0.0012	117.42	.000852±0.00060
65.42	.0305±0.0062	93.61	.00826±0.0054	119.39	.000681±0.00048
67.44	.0164±0.0044				

(d) Inelastic scattering, 2.30-MeV level

28.62	1.41±0.08	71.52	0.077±0.006	109.68	0.00215±0.00190
32.73	2.61±0.06	73.54	.0535±0.0063	111.66	.00189±0.00068
34.79	1.91±0.05	75.56	.0227±0.0045	113.64	.00104±0.00102
36.84	.879±0.035	77.58	.0142±0.0068	115.61	.0019±0.009
38.90	.925±0.036	79.59	.0159±0.0038	117.58	.0028±0.0012
40.95	2.67±0.06	81.67	.0381±0.0072	119.55	.0014±0.0007
43.00	1.77±0.05	83.62	.0225±0.0036	123.49	.00084±0.00042
45.05	.942±0.036	85.62	.0171±0.0027	125.45	.000596±0.000600
47.09	.396±0.023	87.63	.0089±0.0022	127.41	.00043±0.00025
49.14	.465±0.025	89.63	.00497±0.00166	133.29	.00118±0.00042
51.18	.629±0.029	91.64	.0089±0.0021	135.24	.00059±0.00030
53.23	.489±0.026	93.77	.0074±0.0032	137.20	.00045±0.00026
55.27	.225±0.017	95.77	.0038±0.0012	139.15	0
57.30	.123±0.012	97.76	.00097±0.00097	141.10	.00015±0.00015
59.34	.191±0.016	99.76	.00117±0.00068	143.05	0
61.38	.190±0.016	101.75	.0036±0.0014	144.99	.00093±0.00038
63.41	.140±0.013	103.73	.0037±0.0017	146.96	.00109±0.00041
65.44	.052±0.008	105.72	.0055±0.0020	148.88	.00141±0.00047
67.47	.035±0.006	107.70	.0016±0.0007	150.83	.00063±0.00032
69.49	.054±0.008				

TABLE VI. - DIFFERENTIAL CROSS SECTION FOR SCATTERING OF 42-MeV ALPHA PARTICLES FROM TELLURIUM 126

(a) Elastic scattering

Center mass scattering angle, θ_{cm}, deg	Differential cross section, $d\sigma/d\Omega$, mb/sr	Center mass scattering angle, θ_{cm}, deg	Differential cross section, $d\sigma/d\Omega$, mb/sr	Center mass scattering angle, θ_{cm}, deg	Differential cross section, $d\sigma/d\Omega$, mb/sr	Center mass scattering angle, θ_{cm}, deg	Differential cross section, $d\sigma/d\Omega$, mb/sr
8.34	215000±432	43.31	31.5±0.4	63.69	0.692±0.030	93.91	0.0242±0.0032
10.32	111000±311	45.35	15.3±0.2	64.71	.447±0.019	95.90	.0059±0.0019
12.39	61300±231	47.40	9.70±0.23	65.72	.323±0.016	97.90	.0012±0.0005
14.45	31400±165	49.44	10.5±0.09	67.75	.381±0.024	99.89	.0041±0.0013
16.51	18200±126	50.46	10.4±0.09	69.78	.463±0.019	101.88	.0105±0.0018
18.57	9710±92	51.48	7.66±0.10	71.80	.334±0.022	103.87	.0095±0.0020
20.63	4780±65	52.50	6.65±0.07	73.82	.174±0.011	105.85	.0086±0.0016
22.77	2910±27	53.52	4.63±0.06	75.84	.0545±0.0091	107.84	.0025±0.0010
24.83	1920±4	54.54	3.14±0.05	77.85	.0796±0.0078	109.82	.00011±0.00011
26.89	1020±3	55.56	1.80±0.05	79.87	.115±0.009	111.80	.00132±0.00054
28.94	536±2	56.58	1.83±0.04	81.88	.0795±0.0072	113.77	.00300±0.00092
31.00	360±2	57.60	2.02±0.04	83.89	.0475±0.0042	115.75	.00330±0.00086
33.05	261±1	58.61	2.24±0.04	85.90	.0099±0.0026	117.72	.00280±0.00077
35.11	142±1	60.65	2.18±0.04	87.90	.0117±0.0023	119.69	.00167±0.00061
37.16	73.6±0.5	61.66	1.79±0.04	89.91	.0239±0.0040	121.66	.00042±0.00029
39.21	55.1±0.6	62.68	1.25±0.03	91.91	.034±0.003	123.63	.00024±0.00024
41.26	47.3±0.4						

(b) Inelastic scattering, 0.633-MeV level

22.78	11.7±0.4	51.49	0.309±0.021	69.79	0.058±0.007	97.92	0.0122±0.0018
24.83	8.49±0.3	52.51	.450±0.020	71.81	.0224±0.0060	99.90	.00653±0.00169
26.89	13.8±0.4	53.53	.639±0.025	73.83	.0940±0.0087	101.89	.00415±0.00117
28.95	13.9±0.4	54.55	.775±0.026	75.85	.0660±0.0103	103.88	.00131±0.00076
31.01	7.53±0.30	56.59	.774±0.026	77.87	.0831±0.0082	105.87	.00193±0.00079
33.06	2.79±0.13	57.61	.563±0.024	79.88	.0217±0.0051	107.85	.00396±0.00132
35.11	4.34±0.16	58.63	.349±0.017	81.89	.00419±0.00171	109.83	.00343±0.00104
37.17	5.53±0.13	59.64	.100±0.012	83.90	.0132±0.0039	111.81	.00289±0.00082
39.22	3.50±0.14	60.66	.092±0.009	85.91	.0309±0.0026	113.79	.00189±0.00072
41.27	1.12±0.06	61.68	.120±0.012	87.92	.0247±0.0036	115.76	.00115±0.00051
43.32	1.37±0.08	62.69	.172±0.012	89.92	.0085±0.0024	117.73	.00079±0.00042
45.36	2.10±0.08	63.71	.265±0.019	91.92	.00479±0.00128	119.71	.00118±0.00053
47.41	1.81±0.01	64.72	.294±0.016	93.92	.00296±0.00115	121.67	.00215±0.00069
49.45	.795±0.028	65.74	.304±0.016	95.92	.00750±0.00225	123.64	.00177±0.00065
50.47	.448±0.020	67.76	.121±0.014				

(c) Inelastic scattering, 2.38-MeV level

10.41	38±5	47.44	0.331±0.045	65.77	0.0382±0.0055	95.96	0.00270±0.00141
12.48	19.4±3.7	49.48	.370±0.019	67.80	.0223±0.0060	97.95	.00259±0.00082
14.54	11.0±2.7	50.50	.416±0.019	69.83	.0528±0.0065	99.94	.00044±0.00044
16.61	8.45±2.34	51.52	.370±0.023	71.85	.0497±0.0089	101.93	.00250±0.00090
18.67	3.78±1.54	52.55	.378±0.018	73.87	.0369±0.0054	103.92	.00219±0.00098
20.73	9.54±2.46	53.57	.271±0.016	75.89	.0113±0.0043	105.91	.00238±0.00089
22.79	5.22±0.81	54.59	.219±0.014	77.91	.0161±0.0036	107.89	.00264±0.00108
28.97	1.84±0.14	55.61	.125±0.013	79.92	.0170±0.0027	109.87	.00219±0.00083
33.08	2.20±0.12	56.62	.109±0.010	81.93	.0175±0.0035	111.85	.00116±0.00052
35.14	1.21±0.85	57.64	.131±0.011	83.94	.0130±0.0021	113.82	.00143±0.00063
37.19	.802±0.049	58.66	.159±0.012	85.95	.00562±0.00199	115.80	.000706±0.000408
39.24	.855±0.711	60.70	.166±0.012	87.96	.00880±0.00260	117.77	.00145±0.00057
41.29	.976±0.054	61.71	.123±0.011	89.96	.00775±0.00164	119.74	.000696±0.000399
43.34	.804±0.069	62.73	.156±0.012	91.96	.00707±0.00205	121.71	.00102±0.00047
45.39	.541±0.040	63.74	.084±0.011	93.96	.00329±0.00108	123.69	.000350±0.000284

TABLE VII. - DIFFERENTIAL CROSS SECTION FOR SCATTERING OF 42-MeV ALPHA PARTICLES FROM TELLURIUM 128

(a) Elastic scattering

Center mass scattering angle, θ_{cm}, deg	Differential cross section, $d\sigma/d\Omega$, mb/sr	Center mass scattering angle, θ_{cm}, deg	Differential cross section, $d\sigma/d\Omega$, mb/sr	Center mass scattering angle, θ_{cm}, deg	Differential cross section, $d\sigma/d\Omega$, mb/sr	Center mass scattering angle, θ_{cm}, deg	Differential cross section, $d\sigma/d\Omega$, mb/sr
8.25	269000±667	30.55	425±2	48.99	12.3±0.1	67.29	0.414±0.046
10.30	125000±455	32.60	320±3	51.03	9.58±0.08	69.32	.524±0.061
12.36	67100±334	34.65	168.0±0.4	53.07	4.54±0.06	71.34	.412±0.013
14.42	34300±239	36.71	86.2±0.4	55.10	2.17±0.07	73.36	.206±0.038
16.48	19600±180	38.76	64.7±0.2	57.14	2.41±0.04	75.38	.0702±0.0056
18.54	10500±132	40.80	57.8±0.3	59.18	2.60±0.08	77.40	.121±0.029
20.60	5060±92	42.85	36.0±0.2	61.21	1.89±0.04	79.41	.132±0.0077
24.38	2260±7	44.90	17.3±0.2	63.24	.802±0.043	81.42	.0860±0.0248
26.44	1230±4	46.94	11.5±0.1	65.27	.350±0.017	83.43	.0390±0.0042
28.49	625±4						

(b) Inelastic scattering, 0.740-MeV level

20.27	21.7±0.7	36.71	4.97±0.09	53.08	0.561±0.022	69.33	0.0381±0.0171
22.33	12.2±0.4	38.77	3.72±0.06	55.12	.681±0.040	71.36	.0253±0.0035
24.39	5.22±0.33	40.81	1.04±0.04	57.15	.492±0.021	73.38	.130±0.032
26.44	10.8±0.4	42.86	1.22±0.03	59.19	.152±0.019	75.40	.0962±0.0068
28.50	13.2±0.5	44.91	1.90±0.05	61.22	.103±0.009	77.41	.0846±0.0255
30.56	7.22±0.31	46.95	1.69±0.04	63.25	.246±0.025	79.43	.0173±0.0029
32.61	2.83±0.24	49.00	.676±0.032	65.28	.258±0.015	83.45	.0164±0.0028
34.66	4.42±0.06	51.04	.299±0.014	67.31	.183±0.031		

(c) Inelastic scattering, 1.48-MeV level

26.45	0.775±0.100	40.83	0.143±0.015	55.13	0.0276±0.0042	71.37	0.0143±0.0026
28.51	.940±0.138	42.87	.144±0.011	57.17	.0189±0.0040	75.41	.0033±0.0013
30.56	1.07±0.12	44.92	.074±0.011	59.20	.0246±0.0039	77.43	.0077±0.0077
32.62	.696±0.119	46.97	.049±0.006	61.24	.0293±0.0050	79.44	.0043±0.0014
34.67	.547±0.021	49.01	.059±0.009	63.27	.0260±0.0041	81.46	.0077±0.0077
36.72	.220±0.018	51.05	.066±0.006	65.30	.0104±0.0030	83.47	.0053±0.0016
38.78	.254±0.015	53.09	.049±0.006	67.32	.0269±0.0120		

(d) Inelastic scattering, 2.44-MeV level

20.28	1.12±0.15	38.79	0.813±0.026	53.11	0.158±0.012	65.33	0.0242±0.0046
22.34	3.22±0.20	40.84	.677±0.032	55.15	.127±0.009	67.34	.0322±0.0132
24.40	1.43±0.17	42.89	.697±0.024	57.19	.103±0.009	71.39	.0457±0.0047
28.52	1.51±0.18	44.94	.440±0.026	59.22	.107±0.008	75.43	.0158±0.0028
32.63	1.31±0.16	46.98	.315±0.016	61.26	.0931±0.0090	79.47	.0125±0.0025
34.68	1.35±0.03	49.03	.304±0.022	63.29	.0677±0.0065	83.49	.0169±0.0029
36.74	.294±0.021	51.07	.281±0.013				

TABLE VIII. - DIFFERENTIAL CROSS SECTION FOR SCATTERING OF 42-MeV ALPHA PARTICLES FROM TELLURIUM 130

(a) Elastic scattering

Center mass scattering angle, θ_{cm}, deg	Differential cross section, $d\sigma/d\Omega$, mb/sr	Center mass scattering angle, θ_{cm}, deg	Differential cross section, $d\sigma/d\Omega$, mb/sr	Center mass scattering angle, θ_{cm}, deg	Differential cross section, $d\sigma/d\Omega$, mb/sr	Center mass scattering angle, θ_{cm}, deg	Differential cross section, $d\sigma/d\Omega$, mb/sr
8.24	239000±500	28.60	513±1	51.13	7.51±0.053	73.46	0.131±0.0062
10.30	107000±300	30.66	357±2	53.17	4.04±0.043	75.48	.0659±0.0044
12.36	58800±230	32.71	263±1	55.20	1.82±0.026	77.49	.0898±0.0055
14.44	30400±170	34.76	143±0.6	57.24	2.13±0.031	79.51	.124±0.0065
16.48	17900±130	36.81	76.7±0.40	59.27	2.31±0.029	81.52	.0857±0.0055
18.32	10200±104	38.86	57.4±0.36	61.31	1.52±0.020	83.53	.0387±0.0039
18.54	9210±92	40.91	50.2±0.32	63.34	.649±0.016	85.54	.0171±0.0025
20.60	4360±64	42.96	30.8±0.26	65.36	.294±0.009	87.54	.0294±0.0034
22.44	2970±4	45.00	14.2±0.080	67.39	.452±0.012	89.54	.0368±0.0036
24.49	1820±8	47.05	9.97±0.15	69.41	.519±0.012	91.55	.0275±0.0033
26.55	1030±3	49.09	10.5±0.069	71.44	.362±0.010		

(b) Inelastic scattering, 0.840-MeV level

22.44	4.44±0.15	40.92	0.743±0.039	59.29	0.0787±0.0054	77.51	.0342±0.0036
24.50	5.61±0.46	42.97	.682±0.039	61.32	.0547±0.0037	79.52	.0115±0.0019
26.56	6.09±0.18	45.01	1.11±0.022	63.35	.145±0.0074	81.54	.00319±0.0011
28.61	6.77±0.12	47.06	.928±0.045	65.38	.150±0.0069	83.55	.0111±0.0021
30.67	3.57±0.14	49.10	.417±0.014	67.41	.0880±0.0051	85.55	.0121±0.0021
32.72	1.54±0.057	51.14	.175±0.0081	69.43	.0228±0.0024	87.56	.0143±0.0024
34.77	2.30±0.071	53.18	.322±0.012	71.45	.0152±0.0021	89.56	.00536±0.0014
36.82	3.05±0.080	55.22	.417±0.012	73.47	.0407±0.0034	91.56	.00120±0.00069
38.87	2.00±0.066	57.26	.282±0.011	75.49	.0574±0.0041		

(c) Inelastic scattering, 1.59-MeV level

28.62	0.143±0.017	42.98	0.0796±0.013	55.23	0.0112±0.0020	67.42	0.00232±0.00082
30.67	.305±0.040	45.03	.0404±0.0043	57.27	.00770±0.0019	71.47	.00525±0.0012
32.73	.167±0.019	47.07	.0399±0.0094	59.30	.0112±0.0021	73.49	.00707±0.0013
34.78	.176±0.020	49.11	.0189±0.0029	61.34	.0115±0.0017	75.51	.00293±0.00093
36.83	.175±0.019	51.16	.0242±0.0030	63.37	.00977±0.0019	77.53	.00377±0.0012
38.88	.0882±0.014	53.19	.0199±0.0030	65.40	.00596±0.0014	79.54	.00215±0.00083
40.93	.0774±0.013						

(d) Inelastic scattering, 2.73-MeV level

22.46	1.59±0.092	43.00	0.387±0.029	55.24	0.0425±0.0040	67.45	0.0177±0.0023
26.57	.496±0.051	45.04	.159±0.0084	57.29	.0512±0.0048	71.50	.0195±0.0024
30.69	1.15±0.079	47.09	.135±0.017	59.33	.0715±0.0052	73.52	.0116±0.0017
34.80	.449±0.031	49.13	.146±0.0081	61.36	.0546±0.0037	75.54	.00614±0.0013
36.85	.248±0.023	51.18	.159±0.0077	63.39	.0282±0.0033	77.55	.00411±0.0012
38.90	.357±0.028	53.22	.102±0.0068	65.42	.00959±0.0018	79.57	.00628±0.0013
40.95	.491±0.032						

TABLE IX. - EQUIVALENT OPTICAL MODEL POTENTIALS FOR TELLURIUM 126

Nuclear radius constant, R_o	Strength of nuclear optical potential		Diffuseness parameter in Woods-Saxon potential, a	Goodness of fit, χ^2	Total reaction cross section, σ_r	Constant strength of nuclear of optical potential	
	Real, V	Imaginary, W				Real, C_V	Imaginary, C_W
1.18	390.0	130.0	0.6725	127.06	1859	1.13	0.84
1.19	350.0	125.0	.6764	107.7	1865	1.03	.81
1.20	322.5	126.8	.6779	89.2	1879	1.01	.88
1.21	290.0	120.0	.6822	86.9	1885	.925	.85
1.22	275.0	115.0	.6798	92.7	1887	.99	.91
1.23	258.8	103.8	.6776	89.83	1881	1.02	.91
1.24	241.0	96.31	.6774	90.19	1880	1.02	.90
1.25	220.0	90.00	.6796	86.07	1884	.98	.88
1.26	200.5	84.13	.6821	86.88	1886	.91	.86
1.28	177.2	73.54	.6789	89.18	1884	1.00	.92
1.297	150.0	65.25	.6848	87.30	1889	.85	.82
1.30	157.1	64.00	.6748	94.21	1881	1.09	.99
1.32	129.7	56.04	.6812	88.08	1888	.94	.90
1.33	119.1	52.19	.6829	85.91	1890	.91	.88
1.34	111.8	48.87	.6811	88.54	1888	.94	.91
1.35	105.0	45.00	.6794	90.32	1885	.98	.97
1.36	101.0	39.82	.6736	108.1	1873	1.10	.96
1.363	100.0	39.00	.6716	111.82	1872	1.11	.96
1.37	94.00	41.12	.6741	96.20	1890	1.08	1.04
1.38	86.00	36.00	.6755	98.25	1880	1.03	.96
1.39	76.06	35.21	.6837	95.50	1892	.99	1.02
1.40	73.49	32.23	.6769	96.28	1885	1.00	.97
1.42	63.04	29.34	.6786	87.58	1895	.98	1.01
1.427	60.00	28.00	.6779	88.56	1895	.98	1.01
1.44	54.40	26.49	.6789	91.30	1901	.98	1.06
1.449	50.00	25.00	.6811	96.34	1902	.95	1.05
1.46	45.87	23.54	.6815	93.34	1905	.92	1.04
1.479	40.00	21.50	.6820	87.84	1911	.86	1.02
1.48	39.65	21.55	.6824	84.64	1915	.91	1.09
1.50	34.92	19.61	.6813	82.08	1921	.93	1.16
1.52	31.11	18.04	.6787	80.94	1931	1.02	1.31
1.54	27.96	16.39	.6737	80.80	1941	1.13	1.48
1.56	25.21	14.75	.6686	88.54	1943	1.33	1.73
1.58	22.74	13.44	.6629	95.64	1949	1.52	2.00
1.60	20.62	11.93	.6553	102.6	1950	1.84	2.37
1.62	18.72	10.60	.6471	114.1	1949	2.24	2.83
1.64	17.01	9.37	.6384	128.0	1947	2.88	3.52